Consistency of Aerosol Size Distributions Inferred from Measurements of Solar Radiation and Aerosols

By Teruyuki Nakajima, Tamio Takamura[1], Maki Yamano[5] and Masataka Shiobara[2]

Upper Atmosphere Research Laboratory, Tohoku University, Sendai 980, Japan

Toyotaro Yamauchi[3], Ryozo Goto[4] and Keizo Murai[6]

Meteorological Research Institute, Tsukuba 305, Japan
(Manuscript received 24 March 1986, in revised form 2 July 1986)

Abstract

Measurements of direct and diffuse solar radiations were carried out in cooperation with in situ measurements of aerosols during two periods of Nov. 4–7, 1978 and Nov. 1–3, 1979 in Sendai, Japan. Intercomparison of volume spectra of aerosols obtained by several kinds of instruments showed that bimodal volume spectra are preferred to interpret the observed data. Values of the complex refractive index of aerosols were also investigated using a polar nephelometer and the diffuse to global radiation ratio measured by spectro-pyranometers.

1. Introduction

Knowledge on the size distribution and the complex refractive index of aerosols is very important to know the radiative effects of aerosols on the heat budget of the atmosphere and on our optical environment. In the last two decades, many instruments and techniques to obtain these quantities have been developed. Popular methods among these are in situ aerosol measurements by using impactors and particle counters and indirect optical soundings by radiometers. Although agreement of results from these methods was verified in simultaneous measurement programs, *e.g.* aerosol-radiation

Present Affiliations and Addresses:
1) Institute of Geoscience and Astronomy, The National Defence Academy, Yokosuka 239, Japan.
2) Meteorological Research Institute, Tsukuba 305, Japan.
3) Meteorological College, Kashiwa 277, Japan.
4) Office of Instrument, Japan Meteorological Agency, Tokyo 100, Japan.
5) Higashi 5-29-14, Koganei, Tokyo 184, Japan.
6) Kitazawa 4-12-11, Setagaya, Tokyo 155, Japan.

research programs of CANEX (Kondratyev *et al.*, 1974) and GAARS (DeLuisi *et al.*, 1976), lidar-aircraft intercomparisons (Reagan *et al.*, 1977), and aerosol-radiation measurements (Russell *et al.*, 1979), some characteristic errors in the methods have been noticed. Calculated optical thickness of aerosols with the size distribution estimated from in situ aerosol measurements was systematically smaller than that observed by spectro-pyrheliometers in some cases (DeLuisi *et al.*, 1976; Reagan *et al.*, 1977). As for the complex refractive index of aerosols, it is very difficult to assess agreement among results from in situ samplings and indirect soundings, due to large errors involved in these methods (WCP report, 1983).

Since we developed an estimation technique of the complex refractive index of aerosols by a polar nephelometer (Tanaka *et al.*, 1982) and of the columnar volume spectrum by an aureolemeter (Nakajima *et al.*, 1983), we analyze in this paper the data obtained in a measurement program of solar radiation and aerosols using a polar nephelometer and an aureolemeter with

radiometers and particle counters, carried out in 1978 and 1979 for comparison of the volume spectrum and the refractive index of aerosols obtained by several methods and for investigation of consistency of the observed data with each other. Because our interest is in the interaction of solar radiation with aerosols, we try to get a model of the volume spectrum and complex refractive index to interpret the observed aerosol characteristics concerning the solar radiative transfer, *i.e.* the optical thickness, phase function and single scattering albedo.

2. Measurement system

Instruments joining this program and physical quantities measured by these instruments are shown in Fig. 1. Instruments are classified into two groups, *i.e.* those to measure the solar radiation and those to measure aerosols.

2.1 Measurements of solar radiation

The direct solar radiation F_λ at a wavelength λ was measured by a spectro-pyrheliometer which is composed of a double monochromator and an automatic sun follower. The viewing angle of the instrument is about $2°$ corresponding to the entrance slit width of 0.5 mm with dispersion of 33 Å. Radiative intensity in the spectral range from 350 nm to 2000 nm can be measured by a photomultiplier and a PbS cell.

The direct solar radiation was also measured by a sunphotometer (Model MS-110, EKO Instruments Co.) in the observation in 1979. The sunphotometer has a full viewing angle of $2.25°$ and five interference filters with peak transmission wavelengths (half widths) of 369(6),

500(5), 675(4), 776(5) and 862(6) nm. The optical thickness of aerosols τ_λ was calculated by signals of the instruments calibrated by the Langley method.

Diffuse and global fluxes of solar radiation, D_λ and G_λ, were respectively measured by a spectro-pyranometer with and without an automatic shading disk to block the direct solar radiation. The spectrometer is the same as the one used in the spectro-pyrheliometer with an integrating sphere to integrate the global radiation.

Circumsolar light intensities were measured by an aureolemeter A of the group of Meteorological Research Institute in 1978 and by an aureolemeter B of the group of Tohoku University in 1979. The aureolemeter A is composed of a telescope with viewing angle less than $1°$ and a double monochromator, and scans the meridional plane of the sun. The aureolemeter B is a telescope mounted on an equatorial on a horizontal turntable and scans the circle of the solar almucanter. Circumsolar intensities of radiation at scattering angles $\Theta \geq 2°$ were measured at $\lambda = 560$, 788 and 1040 nm by a silicon photo-diode and three interference filters. Measured circumsolar intensities $I_\lambda(\theta, \phi)$ were processed to get the forward part of the phase function of aerosols $P(\Theta)$ by removal of multiple-scattering radiation.

2.2 Measurements of aerosols near the ground surface

In situ measurements of aerosols near the ground surface were done by the instruments in the group (II) in Fig. 1. Polar nephelometer

Instruments	Periods			Measured quantities	Analyses
	NOV.1978 5 6 7	1979 1 2			
(I)					
Spectro-pyranometer	* *	* *		G_λ	D_λ/G_λ —*radiative transfer*→
– with shading ring	* *	* *		D_λ	
Spectro-pyrheliometer	* *	* *		F_λ	τ_λ —*inversion*→
Sunphotometer		* *		F_λ	
Aureolemeter	* *	* *		$I_\lambda(\theta,\phi)$	$P(\Theta)$ —*inversion*→
(II)					
Polar nephelometer	* * *	* *		$P_1(\Theta), P_2(\Theta)$	*inversion*
Optical particle counters		* *		$n(r)$	
Whitby aerosol analyzer		* *		$n(r)$	
Andersen sampler		* *		$m(r)$	$\tilde{m}$, dV/dlnr
Filter sampler		* *		$n(r)$	

Fig. 1 Schematic diagram of the measurement system.

measures differential cross sections, or phase functions $P_1(\Theta)$ and $P_2(\Theta)$, for radiations polarized perpendicularly and parallelly to the scattering plane, respectively, at scattering angles $7° \leq \Theta \leq 170°$ at the wavelength of 514 nm (Takamura and Tanaka, 1978).

Particle counters were introduced in 1979 as in Minnesota Aerosol Analyzer System (Husar et al., 1972) to obtain size distributions of aerosols effective on the radiative transfer. Two optical particle counters, Model KC-01 (RION Co.) and PM-730 (Dan Industrial Co.) have 5 and 15 discriminating stages, respectively, at particle radii from 0.15 to about 3 μm. A Whitby-type aerosol analyzer Model 3030 (Nihon Kagaku Kogyo Co.) was used to count particles smaller than 0.2 μm. This instrument electro-statically counts particles at 11 discriminating radii from 0.0016 to 0.5 μm. The number spectrum of aerosols $n(r) = dN/dr$, where N is the cumulative number density of aerosols at the particle radius r, was determined by these counters.

In addition to these counters, an 8-stage Andersen sampler and a Nuclepore filter sampler were used to obtain the mass spectrum $m(r)$ and samples for a morphological analysis by images of a scanning electron microscope (SEM). An aerosol holder with a Nuclepore filter of 0.05 μm pore size was put out of the window and pumped for about 5 to 7 hours with flow rate of 0.35 liter/min/cm^2. Sampling by the Andersen sampler was taken once a day with sampling time of about 24 hr (9:00–8:30 on next day) with the flow rate of 28.3 liter/min. Mass spectrum obtained by the Andersen sampler was converted to the volume spectrum assuming the density of aerosols to be 2 g/cm^3.

Radiometers were set on the top of a building in the campus of Tohoku University located on a hill at about 2 km west of Sendai, Japan (38°15.43'N, 140°50.55'E, 153 m MSL). Particle counters and the polar nephelometer were set in a room of the same building (at about 23 m above the ground) and the sampling air was taken through a flexible tube of 300 mm in diameter and 3 m long, that is wide and short enough to avoid trapping of particles by the tube wall and drying of particles due to warming by the room temperature.

2.3 Analyses

As shown in Fig. 1, the volume spectrum $dV/d\ln r = 4\pi r^4/3\, n(r)$ and the complex refractive index $\widetilde{m}$ of aerosols are estimated from the observed quantities mentioned in the preceding subsections. Simultaneous inversion of the combined data of the optical thickness and the aureole intensity (Nakajima et al., 1983) and the inversion-library method using the polar nephelometer data (Tanaka et al., 1982) are used to retrieve the volume spectrum. As for estimation of the complex refractive index of aerosols, DeLuisi et al. (1976) used the diffuse to direct radiation ratio and Reagan et al. (1977) used the particulate polarization ratio measured by a bistatic lidar. We adopt both methods in essence, using the inversion-library method and the method of diffuse to direct radiation ratio (King, 1979; King and Herman, 1979).

3. Results and discussion

3.1 Time variation of the aerosol concentration

Figure 2 shows time series of the optical thickness τ_{500} at $\lambda = 500$ nm measured by the
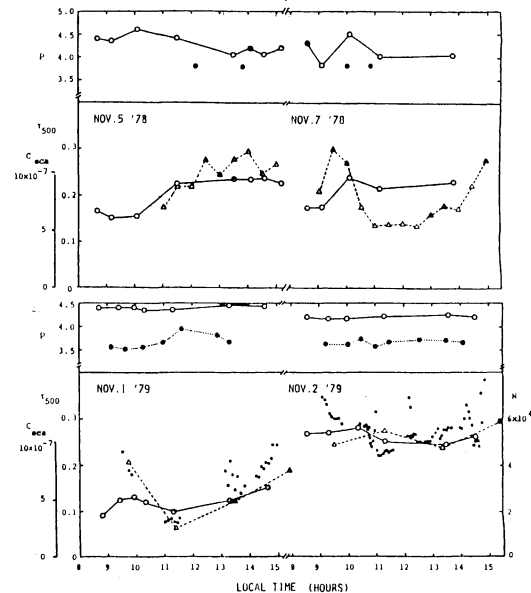
Fig. 2 Time series of the optical thickness at $\lambda = 500$ nm, τ_{500} ($\circ$), scattering coefficient at $\lambda = 514$ nm, C_{sca}/cm ($\triangle$), and total particle number N/liter ($\bullet$). Values of the exponent of the effective power law number spectrum of aerosols, p, estimated from τ_λ and $P(\Theta)$ are shown by $\circ$ and $\bullet$, respectively.

spectral pyrheliometer and the sunphotometer, the scattering coefficient C_{sca} at $\lambda = 514$ nm from the data of the polar nephelometer, and the number of particles N larger than 0.15 μm in radius measured by the optical particle counter PM-730. For the observed cases, the total particle number and the scattering co-efficient near the ground tended to decrease near the noon, whereas the aerosol optical thickness was relatively unchanged. An optically effective scale height τ/e defined by the ratio of the optical thickness to the extinciton co-efficient near the ground was about 2 km at morning and late afternoon for all the cases and somewhat larger at noon as shown in column 11 of Table 1 for eight data sets, which were established so that each set consists of selected data measured at nearly same time. Investigation of vertical temperature profiles at 8:30 and 20:30 JST showed that a temperature inversion was realized at about 1.8 km MSL at 8:30 and 20:30 on Nov. 7, 1978, and at about 2 km MSL at 8:30 on Nov. 1, 1979. Observation by a low altitude radiosonde carried out on Nov. 1, 1979 showed that a stable stratification near the ground broke down until 11:30 with intrusion of dry NW wind of about 3.5 m/s and a weak stable conditon was again realized until 13:30. In Table 1, we show the gradient of the poten-tial temperature, relative humidity and wind velocity near the ground. On Nov. 2, wind of about 3 m/s blew steadily and the atmosphere was in a condition more neutral than on Nov. 1. Diurnal variation of the aerosol concentration at the ground surface was relatively small on

this day. Growth and shrink of the aerosol layer with change of the regime of temperature stratification was one of reasons of the phe-nomenon as investigated by Kobayashi and Yano (1982), although some criticism exists (Kaufman and Fraser, 1983). Well mixed aerosol layer was often realized when temperature inversion existed as reported by several investi-gators (Bridgman, 1979; Spinhirne et al., 1980; Takamura and Miyazaki, 1981).

3.2 Retrieval of the volume spectrum

Since the wavelength dependence of the optical thickness and the scattering angle de-pendence of the forward part of the phase function can be expressed by the exponent p of an effective power law number spectrum, $n(r) = Cr^{-p}$, for smaller and larger particles, respectively (Nakajima et al., 1983), we show values of p in Fig. 2 to interpret the data of τ_λ and $P(\Theta)$. Separation of values of the ex-ponent obtained by these quantities shows some bimodal size distributions were general in these observation periods. This is more clearly shown by volume spectra obtained by several instruments displayed in Fig. 3.

In Fig. 3, columnar volume spectra retrieved from the combined data of τ_λ and $P(\Theta)$ (here-after we refer as $(A+O)$ data) were normalized by the scale height τ/e to adjust the vertical scale. As for the optical counters, data of PM-730 alone were shown, since the results of the two counters were consistent with each other (Takamura, 1986). From the figure, it is found that the general feature of volume spectra was

Table 1   Complex refractive index ($\widetilde{m}$), relative rms deviation (%-err), scale height (τ/e) of the aerosol layer estimated by several methods with the gradient of the potential temperature ($d\theta/dz$), relative humidity (H) and wind velocity (W) near the ground.

| | | Inversion | | | | Bimodal | | | | | | | | |
| | | Nephelometer | A+O | | Nephelometer | | A+O | | | OPC+WAA | τ/e | $d\theta/dz$ | H | W |
Date	Time	$\widetilde{m}$	%-err		$\widetilde{m}$		%-err	C_1/C_2		$\widetilde{m}$	(km)	(K/Km)	(%)	(m/s)
NOV.5 '78	13:50-14:50	1.50-0.01i	4.2	6.1	1.50-0.01i	6.6	10.0	1.4		–	1.9	–	58	2.8NW
NOV.7 '78	10:50-12:00	1.50-0.02i	7.1	7.6	1.55-0.03i	8.6	8.8	1.4		–	3.1	–	46	1.8NW
NOV.1 '79	9:30-10:05	1.55-0.02i	5.1	5.4	1.50-0.01i	7.3	6.0	1.4		1.50-0.01i	1.3	3.4	59	1.6NE
	11:10-11:45	1.50-0.01i	6.6	5.0	1.50-0.01i	8.6	12.0	1.0		1.50-0.01i	3.1	0.3	45	3.5NW
	13:10-13:50	1.55-0.03i	6.3	5.2	1.50-0.01i	7.1	9.0	1.0		1.55-0.01i	2.0	2.6	51	2.0W
NOV.2 '79	9:15- 9:50	1.55-0.05i	7.3	3.3	1.55-0.03i	8.6	15.7	2.1		1.55-0.02i	2.3	2.8	52	3.8N
	11:00-11:40	1.55-0.02i	5.6	6.1	1.55-0.03i	7.5	12.8	2.1		1.60-0.03i	1.8	0.8	39	3.7N
	13:05-13:40	1.55-0.05i	4.3	5.4	1.55-0.03i	7.4	7.2	1.4		1.55-0.02i	2.1	0.5	31	3.0N
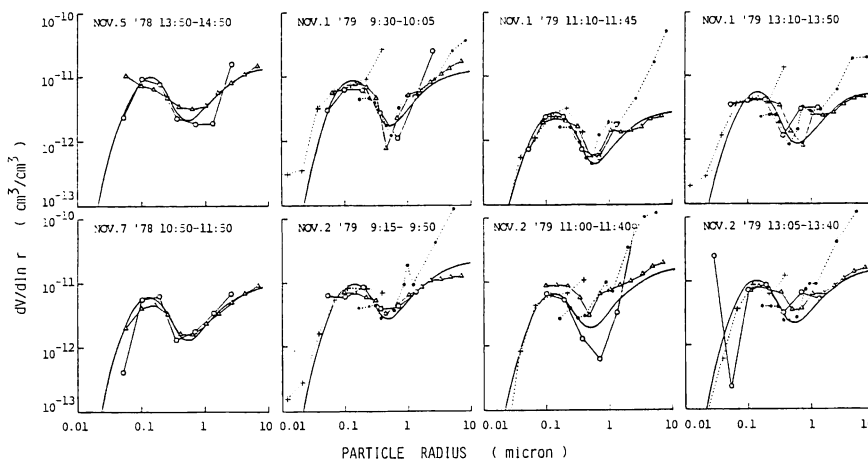
Fig. 3   Volume spectra retrieved from the data of the polar nephelometer (○), the (A+O) data (△), optical particle counter (●) and Whitby counter (+), respectively. Solid lines show model values.

a bimodal profile with a saddle point around the radius of 0.6 μm. It is also found that columnar volume spectra for submicron particles were similar to those near the ground surface although the scale height varied from case to case. This is not so peculiar since the scale height of the aerosol stratification was as small as about 2 km and large portion of aerosols existed in the well mixed lower atmosphere. Spinhirne et al. (1980) showed that 84% of the total optical thickness were attributable to aerosols in the mixed layer in their case study. Several aircraft measurements of the aerosol size distribution showed that the size distribution of aerosols had similar character in the mixed layer (Reagan et al., 1977; Takamura and Miyazaki, 1981; Kobayashi and Yano, 1982). For the case of 11:00−11:40 on Nov. 2, 1979, however, data are not consistent with each other suggesting strong spatial inhomogeneity and/or large time variation of aerosol characteristics.

The volume spectra obtained by the Whitby analyzer and the optical particle counters were not consistent around the radius of 0.2 μm, i.e. around the upper and lower detection limits of the counters. Smoothed curves of both spectra, however, well follow the other profiles. This suggests that the discrepancy between the results of the electro-static analyzer and the optical counters was due to systematic counting errors of both counters.

As for large particles, we find some discrep-ancies among the spectra. Results from the optical counters and the polar nephelometer tend to become large for particle radii larger than 2 μm compared with columnar volume spectra. Some causes are expected. First, this tendency is possible since large particles under discussion would be particles derived from the soil (Patterson and Gillette, 1977) and the volume spectrum near the ground would be larger than the columnar average. We suspect, however, that this is not so realistic because no large systematic variation of the volume spectrum in the mixed layer has been reported as discussed above and the volume spectra obtained by aerosol samplers near the ground also did not show such large values as shown later. Second reason is an overestimation of the absorption index of large particles. Since the optical counters were calibrated by poly-styrene latex spheres with the refractive index of 1.595, we corrected the signals using the refractive index shown in column 3 of Table 1, estimated by the polar nephelometer data, as in Kobayashi and Yano (1982). For large par-ticles, this correction is large and affected se-riously by the estimation error of the refractive index $\tilde{m} = m_r - m_i i$, especially of the absorption index m_i. This is more or less true also for the inversion of the polar nephelometer data. Tend-ency of the discrepancy in Fig. 3 suggests some overestimation of the absorption index m_i for large particles. This is possible because the

inversion-library method (Tanaka et al., 1982) assumes homogeneity of the optical property of aerosol polydispersion, whereas carbon-rich anthropogenic aerosols appear as the accumulation mode of the spectrum at submicron particle radii (Patterson and Gillette, 1977) and the polar nephelometer is more sensitive to the light scattering by submicron particles. The retrieved value of the absorption index is also affected by nonsphericity of aerosols. Asano and Sato (1980) showed that the backscattering of a large spheroid is much smaller than that of the equivalent sphere. Equivalent value of the absorption index increases with an decrease in the backscattering. By these facts, the absorption index m_i of large particles tend to be overestimated. On the other hand, volume spectra for large particles retrieved from the $(A+O)$ data would be more reliable because the inversion of the combined data is sensitive to large particles and little affected by estimation error of the absorption index of large particles (Nakajima et al., 1983). As a conclusion, some discrepancy of the volume spectra for large particles are reduced if we take account an overestimation of the spectra near the ground obtained from the polar nephelometer and optical counters.
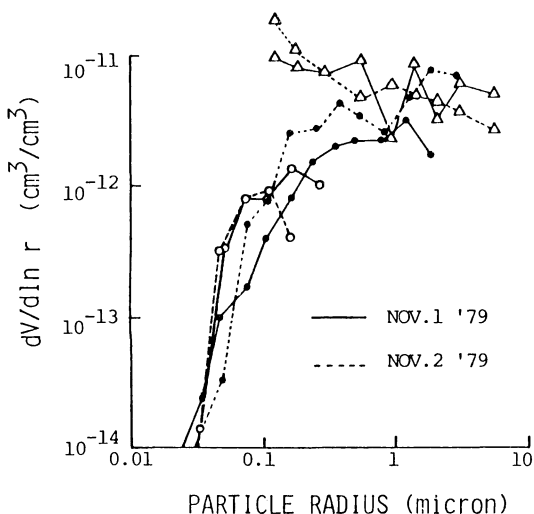
Fig. 4 Volume spectra measured by an Andersen sampler (△) and by a Nuclepore filter (●, ○), respectively. Data on Nov. 1 and Nov. 2, 1979 are shown by solid and broken lines, respectively.

Figure 4 shows the volume spectra obtained by aerosol samplers. From the figure it is found that the concentration of submicron aerosols was largely underestimated compared with the corresponding spectra in Fig. 3. Investigation of SEM images shows that submicron particles often assembled into large irregular particles or adhered to giant particles. Open circles in Fig. 4 show the spectra calculated by assuming these small particles were separately floating in the air. Since such alternation also underestimates small particles, apparent collection efficiency for particles smaller than about 0.2 μm in radius was considerably smaller than the announced specification of the filter, i.e. 100% for particles larger than the pore size (Spurný et al., 1969). Similarly the results from the Andersen sampler failed to detect the bimodal feature of the volume spectra. One of reasons would be that results of the Andersen sampler reflected the daily averaged volume spectra. Degeneration and drying of particles are also serious for these aerosol samplers. Some attentiveness, therefore, must be paid when we utilize the volume spectra obtained by the aerosol samplers to calculate radiative effects by aerosols, because optically effective particle radius is in the range from 0.1 to 1 μm, as small as radii for which these samplers showed large discrepancies.

3.3 Modelling of the volume spectrum

As shown in the preceding subsection, the retrieved volume spectra were consistent with each other apart from some discrepancies originated from systematic estimation errors of the instruments and from difference of sampling airmasses, so that it is useful to fit the spectra to a model to know the essential feature of the volume spectra contributing to the observed quantities. We fit the volume spectra in Fig. 3 to a sum of two log-normal functions as follows;

$$dV/d \ln r$$

$$= \sum_{i=1}^{2} C_i \exp\left\{-\frac{1}{2}[\ln(r/a_i)/\ln s_i]^2\right\}, \quad (1)$$

where C_i, a_i and s_i are the coefficient, mode radius and standard deviation of the mode i of the spectrum, respectively. The mode 1 in

Fig. 3 corresponds to the accumulation mode attributed to the secondary aerosols including anthropogenic aerosols. Reported values of the mode radius and standard deviation for the accumulation mode were $(a_1, s_1) = (0.14, 1.56)$ for the light aerosol loading case of Patterson and Gillette (1977), (0.41, 1.36) and (0.36, 1.58) for the spectra at Morioka and Yokohama, respectively, in winter season observed by Fujimura and Hashimoto (1977), (0.17, 1.61) and (0.19, 1.64) for continental background aerosols and for a typical urban pollutant, respectively, by Slinn (1983), and (0.14, 2.6) for the yearly averaged spectrum effective on the polar nephelometer data (Tanaka et al., 1983). The mode radius varies with various conditions (Fitch and Cress, 1981), while the standard deviation has values around 1.5. We adopt the values of (0.13, 1.8) and (10.0, 4.0) for the modes 1 and 2 of the volume spectrum, respectively taking the above facts into consideration and comparing the observed data with theoretical ones calculated with several model spectra as discussed in Sec. 3.4. For the mode 2, above values are somewhat tentative since our data have no sensitivity to particles as large as 10 μm and detail of the mode 2 of spectra is not important for calculation of radiative transfer characteristics. Moreover, some of the reported volume spectra do not fit to the simple bimodal log-normal function such as in Eq. (1). An equivalent fitting within the radius range less than 10 μm of the trimodal spectra with a mode of giant particles will give a mode radius and standard deviation somewhat larger than the typical values of (2.72, 2.07) for the gigantic mode of Patterson and Gillette (1977) and (2.30, 1.65) of Fujimura and Hashimoto (1977). Larger mode of Slinn (1983)'s spectra for the North Atlantic background and the typical urban pollution do not fit to a log-normal functions and rather have a feature of a power law function.

The most probable values of the coefficients C_1 and C_2 and the complex refractive index are, then, determined by a least square fitting so as to fit simultaneously the data from the polar nephelometer, sunphotometer (or pyrheliometer) and aureolemeter as shown in columns 9 and 6 of Table 1 with relative fitting errors in column 7 for the polar nephelometer data and in column 8 for the $(A+O)$ data. For simplicity of the fitting, we classified values of the ratio C_2/C_1 into three representatives as 1.0, 1.4, 2.1 and 3.0. The model spectra obtained thus are shown by the solid lines in Fig. 3. Comparing the fitting errors with the reconstruction errors of the inversion techniques (in columns 4 and 5 of Table 1), it is seen that these analytic volume spectra do not fail to express the characters of the retrieved spectra. Since the mode 2 of the spectrum hardly affects the polar nephelometer data, fitting functions for large particles rather follow the results of the aureolemeter.
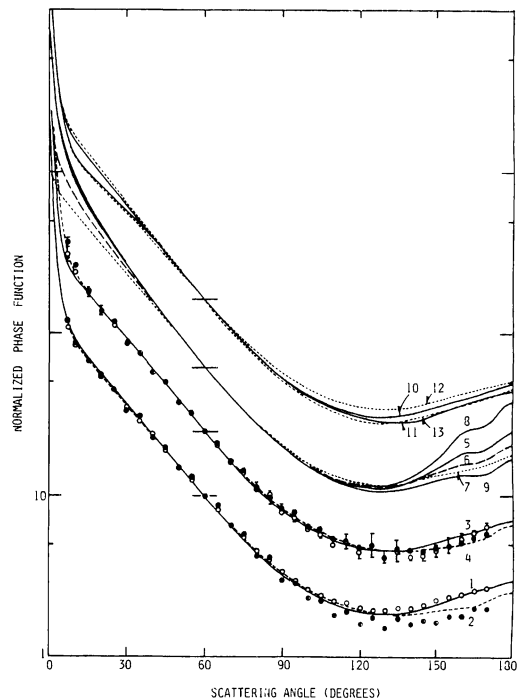
Fig. 5   Observed and model phase functions of aerosols. Profiles 1 to 4 are for data on Nov. 5 (——○——) and Nov. 7, 1978 (- - -●- - -); averages on Nov. 1 (——○——) and Nov. 2, 1979 (- - -●- - -), respectively. Profiles 5 to 9 are models for power law size distributions with $(p, m_i) = (4.0, 0.01), (4.5, 0.01), (5.0, 0.01), (4.0, 0)$ and $(4.0, 0.03)$, respectively, with $m_r = 1.5$. Profiles 10 to 13 are models for bimodal log-normal functions with $(a_1, s_1) = (0.13, 2.0), (0.13, 1.5), (0.1, 1.8)$, and $(0.16, 1.8)$, respectively. Profiles are normalized at $\theta = 60°$.
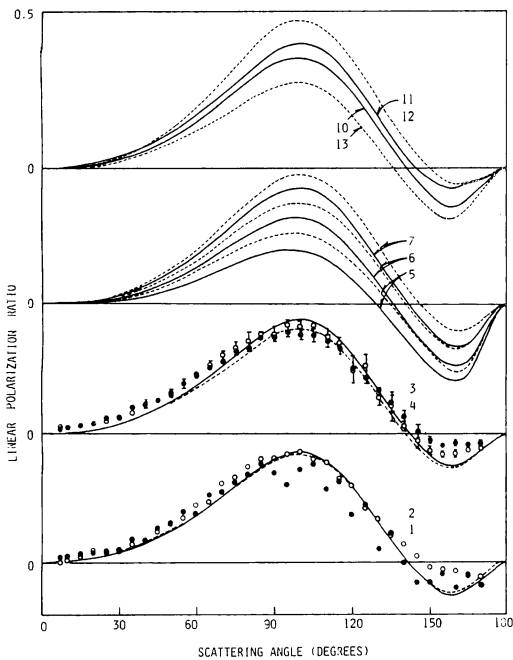
Fig. 6   Same as Fig. 5 but for the linear polarization
    ratios. For profiles 5, 6 and 7, two values of m_i are
    assumed as 0.01 (solid line) and 0.03 (broken line).

3.4   Interpretation of the observed data by the model volume spectrum and refractive index of aerosols

In Figs. 5 and 6, we compare the observed values of the averaged phase function $(P_1 + P_2)/2$ and the linear polarization ratio $(P_1 - P_2)/(P_1 + P_2)$ with those reconstructed using model volume spectra. Some depression of backward scattering of the profile 2 compared with that of the profiles 1 and 3 are attributable to the large absorption index. Although a power law volume spectrum with $p \approx 4.5$ (profile 6 in Fig. 5) is another good approximation for the averaged phase function, the corresponding profile of the linear polarization ratio is too large in magnitude at $\Theta \approx 160°$. The linear polarization ratio is also very sensitive to the parameters of the mode 1 of the bimodal log-normal volume spectrum in Eq. (1). These comparisons show that the adopted model volume spectra are suitable to interpret the polar nephelometer data.

Since the shape of the forward part of the phase function measured by the aureolemeter is scarcely affected by the refractive index,

characteristic profiles are obtained as shown in Fig. 7 by averaging the data sets in 1978, on Nov. 1, 1979, and on Nov. 2, 1979, respectively. The model profiles well follow the observed data including some wavelength dependences. In Fig. 8 we show several profiles of the forward part of the phase function calculated using various volume spectra. It is found that normalized profiles with power law volume spectra are nearly independent of wavelengths, and thus profiles with bimodal ones are more realistic approximation for the observed data. It is also found from Fig. 8 that the forward part of the phase function is sensitive to the value of the ratio C_2/C_1, so that data of the aureolemeter are indispensable for retrieval of the mode 2 of the volume spectra.

Figure 9 shows the observed and model spectra of the optical thickness. It is found that the wavelength dependence of the optical thick-
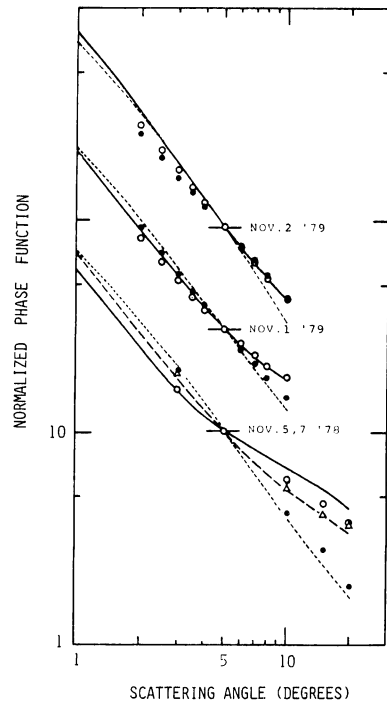
Fig. 7   Observed and model profiles of the forward
    part of the aerosol phase function at $\lambda = 350$
    (—○—), 550 (- - -△- - -) and 1050 nm (- - -●- - -) for
    data in 1978 and at $\lambda = 560$ (—○—) and 1040 nm
    (- - -●- - -) for data in 1979. Profiles are normalized
    at $\Theta = 5°$.
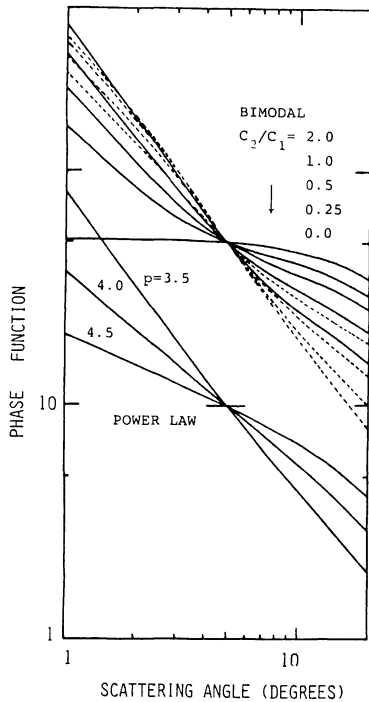
Fig. 8   Model profiles of the forward part of the aerosol phase function. Lower set is for the power law volume spectra with $p = 3.5$, 4.0 and 4.5. Upper set is for the bimodal log-normal volume spectra with $C_2/C_1 = 2$, 1, 0.5, 0.25 and 0 from upper to lower, respectively. Solid and broken lines are at $\lambda = 500$ and 1000 nm, respectively. Profiles are normalized at $\Theta = 5°$.
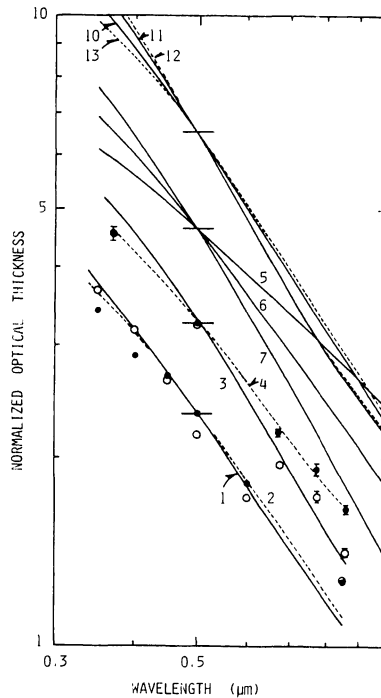
Fig. 9   Observed and model spectra of the optical thickness. Profile nos. and symbols are same as in Fig. 5. Profiles are normalized at $\lambda = 500$ nm.

ness can be simulated by both the log-normal and the power law volume spectra. In this respect, the spectral optical thickness has information on the size distribution less than a combined data with the aureole intensity. If we fit the observed data in Figs. 7 and 9 by a power law volume spectrum, values of p about 3 and 4.3 are suitable, respectively, suggesting prevailing of bimodal volume spectra as discussed in the preceding subsections.

To assess the effect of the size distribution and the refractive index of aerosols on the solar radiative transfer in the observation periods, we show in Table 2 the transmissivity, reflectivity, and ratio of the diffuse to global radiations of homogeneous atmospheres at $\lambda = 500$ nm with various values of the optical airmass m, ratio C_2/C_1, ground albedo A, complex refractive index $\underset{\sim}{m}$, and exponent p if we assume the

power law volume spectrum. With a fixed value of the optical thickness of aerosols, effect of the relative shape of the size distribution is as small as 0.7% of the diffuse to global radiation ratio for the cases in Table 2, so that our estimation scheme of the volume spectrum is sufficiently accurate for calculation of the radiative fluxes. On the other hand, effects of the absorption index and the ground albedo are significant and same order for the cases in the table.

In Fig. 10, the observed diffuse to global radiation ratios are compared with the model value for $C_2/C_1 = 1.4$ as a function of the aerosol optical thickness at $\lambda_{500} = 500$ nm with the optical airmass of 2 and the typical value of the ground albedo of 0.15. Observed values of the diffuse to global radiation ratio in 1978 were consistent with the complex refractive index shown in Table 1, while the data in 1979 were considerably larger than the model values. Unrealistically large value of the ground albedo and/or no absorptivity of aerosols are necessary to interpret the observed values. Since the uncertainty originated from the volume spectrum

Table 2   Transmissivity T, reflectivity R and diffuse to global radiation ratio D/G of homogeneous atmospheres at $\lambda = 500$ nm with various models of aerosols with $\tau_{500} = 0.2$ and $m = 1$, 2 and 3. Figures other than the first row are offset by those of the first row.

			m = 1			m = 2			m = 3		
C_2/C_1	A	m̃	T	R	D/G	T	R	D/G	T	R	D/G
1.4	0.15	1.50-0.01i	0.9165	0.1939	0.2260	0.8020	0.2723	0.3726	0.7096	0.3374	0.4970
2.1			-0.0019	-0.0016	-0.0016	-0.0021	-0.0038	-0.0017	-0.0022	-0.0053	-0.0016
1.0			0.0013	0.0011	0.0011	0.0013	0.0025	0.0010	0.0015	0.0036	0.0011
	0.00		-0.0210	-0.1116	-0.0181	-0.0184	-0.0976	-0.0148	-0.0162	-0.0863	-0.0118
	0.30		0.0219	0.1169	0.0181	0.0192	0.1023	0.0146	0.0170	0.0905	0.0118
	0.45		0.0450	0.2395	0.0362	0.0393	0.2096	0.0293	0.0348	0.1855	0.0235
	0.15	1.50-0.00i	0.0185	0.0113	0.0154	0.0285	0.0218	0.0215	0.0346	0.0300	0.0234
		1.50-0.03i	-0.0205	-0.0118	-0.0176	-0.0309	-0.0226	-0.0252	-0.0372	-0.0311	-0.0278
		1.50-0.05i	-0.0347	-0.0197	-0.0305	-0.0522	-0.0375	-0.0437	-0.0625	-0.0517	-0.0486
		1.55-0.01i	0.0005	0.0018	0.0004	0.0003	0.0035	0.0002	0.0007	0.0045	0.0005
P											
3.5		1.50-0.01i	-0.0045	-0.0065	-0.0038	-0.0017	-0.0166	-0.0013	-0.0015	-0.0227	-0.0011
4.0			0.0025	-0.0011	0.0021	0.0063	-0.0008	0.0049	0.0073	-0.0045	0.0051
4.5			0.0049	0.0019	0.0041	0.0078	0.0035	0.0060	0.0089	0.0055	0.0062
5.0			0.0047	0.0038	0.0040	0.0060	0.0081	0.0047	0.0070	0.0113	0.0049
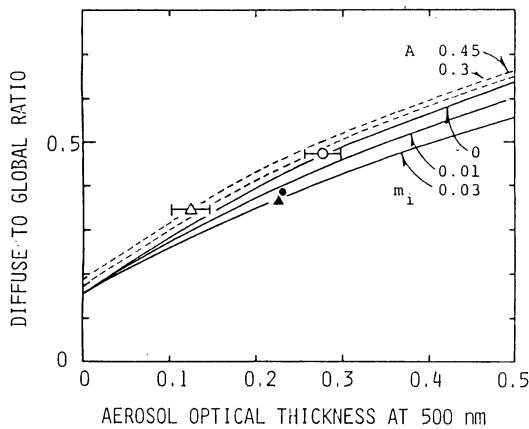
Fig. 10   Diffuse to global radiation ratio for $\lambda = 500$ nm, $m = 2$. Data on Nov. 5 (▲) and Nov. 7, 1978 (●); on Nov. 1 (|—△—|) and Nov. 2, 1979 (|—○—|). $A = 0.15$ for solid lines and $\tilde{m} = 0$ for broken lines.

is small as shown in Table 2, an error in the observed optical thickness is most responsible for this discrepancy. Difference of the optical thicknesses estimated by the pyrheliometer and the sunphotometer is indicated by error bars for the data in 1979. Another cause may be contamination by lights scattered from clouds near the horizon hidden in the haze layer and by obstacles in the field of view of the pyranometer. The above result shows that the diffuse to global radiation ratio is very sensitive to various errors in the measurement.

4. Concluding remarks

In Table 3, we summarize the optical models of aerosols obtained in the preceding analyses with calculated spectra of the single scattering albedo and first two coefficients of the Legendre

expansion of the aerosol phase function, *i.e.* $P(\Theta) = \sum_{n=0}^{\infty} (2n+1)g_n p_n(\cos\Theta)/4\pi$. For calculation of these spectra, we used the bimodal lognormal volume spectrum in Eq. (1) with model values of C_2/C_1 shown in the third row of Table 3. For the coefficients of the Legendre expansion, however, variation of the size distribution in the periods was insignificant, and we show the spectrum with $C_2/C_1 = 1.4$ alone.

The model values of the complex refractive index of aerosols are determined by three different estimates in Table 1. As the third estimation in column 10 of Table 1, we show the optimum value of the complex refractive index to interpret the nephelometer data with synthetic volume spectra of the optical particle counter and the Whitby aerosol analyzer after Takamura (1986). The three estimates of the complex refractive index are consistent with each other and the inversion-library method (Tanaka et al., 1982) may be a good method to estimate the value of the complex refractive index of aerosols.

By these models, the observed quantities were well interpreted with some exception of the diffuse to direct ratio in 1979. Values of the diffuse to global radiation ratio at various optical airmasses will be necessary to attain sufficient ability of estimation of the absorption index as in the method of King and Herman (1979), since the sensitivity of the method is very small as shown in Table 2. Observation of the ground albedo is also necessary to attain accurate estimation of the complex refractive index of aerosols.

Table 3   Model values of the complex refractive index and the ratio C_2/C_1 with calculated spectra of the optical thickness τ, single scattering albedo ω_0, and first and second moments g_1 and g_2 of the Legendre expansion of the phase function at $0.35 \leq \lambda \leq 1$ μm.

date	NOV.5 '78	NOV.7 '78	NOV.1 '79	NOV.2 '79
$\tilde{m}$	1.50-0.01i	1.55-0.03i	1.50-0.01i	1.55-0.03i
C2/C1	1.4	1.4	1.0	2.1
τ_a	$0.229(\lambda/0.5)^{-1.43}$	$0.211(\lambda/0.5)^{-1.38}$	$0.113(\lambda/0.5)^{-1.55}$	$0.245(\lambda/0.5)^{-1.24}$
ω_0	$0.952-0.091\lambda$	$0.891-0.155\lambda$	$0.960-0.093\lambda$	$0.876-0.148\lambda$
g_1	$0.809-0.475\lambda+0.265\lambda^2$			
g_2	$0.616-0.632\lambda+0.438\lambda^2$			

It is found in Table 3 that the absorption index increased on Nov. 7, 1978 and Nov. 2, 1979 compared with those on Nov. 5 and Nov. 1, respectively. The difference would be mainly related to the content of elemental carbon in the atmosphere. It is necessary to measure the content of elemental carbon in cooperation with the techniques discussed in this paper. Such measurement is also required to solve the problem that our estimation of the absorption index of refraction of aerosols (Tanaka et al., 1983) was noticeably larger than that by Grams et al. (1974) in continental areas. This disagreement will be due to difference of the optical property of aerosols and not due to systematic errors in our algorithm. The concentration of elemental carbon in suburban areas in Japan is 2 to 3 times larger than those in areas remote from the urban areas in USA (Ohta and Okita, 1984).

As a future problem, we must improve the accuracy of each instrument. Improved measurements will clear some confusion of our analyses due to systematic errors involved in each data.

Acknowledgments

References

Asano, S. and M. Sato, 1980: Light scattering by randomly oriented spheroidal particles. Appl. Opt., 19, 962–974.

Bridgman, H.A., 1979: Aerosol extinction at 500 nm in urban and rural air at Milwaukee in April 1979. J. Appl. Meteor., 18, 105–116.

DeLuisi, J.J., P.M. Furukawa, D.A. Gillette and B.G. Schuster, R.J. Charlson, W.M. Porch, R.W. Fegley, B.M. Herman, R.A. Rabinoff, J.T. Twitty and J.A. Weinman, 1976: Results of a comprehensive atmospheric aerosol-radiation experiment in the southwestern United States. Part I: Size distribution, extinction optical depth and vertical profiles of aerosols suspended in the atmosphere. J. Appl. Meteor., 15, 441–463.

Fitch, B.W. and T.S. Cress, 1981: Measurements of aerosol size distributions in the lower troposphere over Northern Europe. J. Appl. Meteor., 20, 1119–1128.

Fujimura, M. and Y. Hashimoto, 1977: Estimation of emission sources of trace elements in an atmospheric aerosol by particle size distribution. J. Chem. Soc. Japan, 6, 902–906.

Grams, G.W., I.H. Blifford, Jr., D.A. Gillette and P.B. Russell, 1974: Complex index of refraction of airborne soil particles. J. Appl. Meteor., 13, 459–471.

Husar, R.B., K.T. Whitby and B.Y.H. Liu, 1972: Physical mechanisms governing the dynamics of Los Angeles smog aerosol. Aerosol and Atmospheric Chemistry, G.M. Hidy, Ed., Academic Press, 271–284.

Kaufman, Y.J. and R.S. Frazer, 1983: Light extinction by aerosols during summer air pollution. J. Clim. Appl. Meteor., 22, 1694–1706.

King, M.D. and B.M. Herman, 1979: Determination of the ground albedo and the index of absorption of atmospheric particles by remote sensing. Part I: Theory. J. Atmos. Sci., 36, 163–173.

———, 1979: Determination of the ground albedo and the index of absorption of atmospheric particulates by remote sensing. Part II: Application. J. Atmos. Sci., 36, 1072–1083.

Kobayashi, T. and N. Yano, 1982: The relation between observed aerosol optical thickness and calculated values from size distribution measurements. *J. Meteor. Soc. Japan*, **60**, 1249–1258.

Kondratyev, K. Ya., O.B. Vassilyev, V.S. Grishechkin and L.S. Ivlev, 1974: Spectral radiative flux divergence and its variability in the troposphere in the 0.4–2.4 micron. *Appl. Opt.*, **13**, 478–486.

Nakajima, T., M. Tanaka and T. Yamauchi, 1983: Retrieval of the optical properties of aerosols from aureole and extinction data. *Appl. Opt.*, **22**, 2951–2959.

Ohta, S. and T. Okita, 1984: Measurements of particulate carbon in urban and marine air in Japanese area. *Atmos. Environ.*, **18**, 2439–2445.

Patterson, E.M. and D.A. Gillette, 1977: Commonalities in measured size distributions for aerosols having a soil-derived component. *J. Geophys. Res.*, **82**, 2074–2082.

Reagan, J.A., J.D. Spinhirne, D.M., Byrne, D.W. Thomson, R.G. de Pena and Y. Mamane, 1977: Atmospheric particulate properties inferred from lidar and solar radiometer observations compared with simultaneous in situ aircraft measurements: A case study. *J. Appl. Meteor.*, **16**, 911–928.

Russell, P.B., J.M. Livingston and E.E. Uthe, 1979: Aerosol-induced albedo change: Measurement and modeling of an incident. *J. Atmos. Sci.*, **36**, 1587–1608.

Slinn, W.G.N., 1983: Source and surface-area distributions of atmospheric particles. *Atmos. Environ.*, **17**, 2363–2364.

Spinhirne, J.D., J.A. Reagan and B.M. Herman, 1980: Vertical distribution of aerosol extinction cross section and inference of aerosol imaginary index in the troposphere by lidar technique. *J. Appl. Meteor.*, **19**, 426–438.

Spurný, K.R., J.P. Lodge, Jr., E.R. Frank and D.C. Sheesley, 1969: Aerosol filtration by means of Nuclepore filters: Structural and filtration properties. *Environ. Sci. Technol.*, **3**, 453–464.

Takamura, T. and M. Tanaka, 1978: Measurements of intensity and degree of polarization of light scattered by aerosols. *Sci. Rep. Tohoku Univ.*, *Ser. 5*, **25**, 169–196.

———— and M. Miyazaki, 1981: Measurements of the vertical and horizontal profiles of aerosols over the Pacific ocean near Japan islands. *Sci. Eng. Rep. of the National Defence Academy*, **19**, 1–14.

————, 1986: Reliability of the measured size distribution of aerosols on the light scattering and estimation of complex index of refraction (in preparation).

Tanaka, M., T. Nakajima and T. Takamura, 1982: Simultaneous determination of complex refractive index and size distribution of airborne and water-suspended particles from light scattering measurements. *J. Meteor. Soc. Japan*, **60**, 1259–1272.

————, ———— and ————, 1983: Refractive index and size distribution of aerosols as estimated from light scattering measurements. *J. Clim. Appl. Meteor.*, **22**, 1254–1261.

WCP, 1983: *Report of the experts meeting on aerosols and their climate effects.* A. Deepack and H.E. Gerber, Eds.

太陽放射とエアロゾルの測定から推定されたエアロゾルの粒径分布の整合性

中島映至・高村民雄[1] 山野　牧[5]・塩原匡貴[2]

東北大学超高層物理学研究施設

山内豊太郎[3]・後藤良三[4]・村井潔三[6]

気　象　研　究　所

　太陽直達光と散乱光の観測をエアロゾルの直接測定とあわせて，1978年11月4～7日と1979年11月1～3日の期間，仙台にておこなった。各種の測器から得られた体積スペクトルを相互比較したところ，二山型の体積スペクトルが観測データを説明するために適切であることがわかった。同時に，ポーラー・ネフロメーターと，分光水平面日射計で計られた散乱／全天日射量比とから得られるエアロゾルの複素屈折率についても調べた。

現在所属
(1)　防衛大学校地学教室
(2)　気象研究所
(3)　気象大学校
(4)　気象庁測器室
(5)　東京都小金井市東町 5 —29—14
(6)　東京都世田谷区北沢 4 —12—11